Applied Energy Symposium 2021: Low carbon cities and urban energy systems
September 4-8, 2021, Matsue, Japan
Paper ID: 50

Impact of series circuit layout on the output power performance of thermoelectric generator

Wei He*, Zihan Cai, Chenchen Pei, Xinqiao Wang, Hailong Li, Jian Liu

Tianjin Key Laboratory of Refrigeration Technology, Tianjin University of Commerce, Tianjin 300134, PR China
*Correspondence: weihe@tjcu.edu.cn; Tel.: +86-15122779808

ABSTRACT

To explore the influence of circuit layout on the performance of a thermoelectric generator (TEG), this study utilizes Fortran software to establish the engine exhaust of the thermoelectric generation model, and analyze the temperature distribution of the hot and cold ends of the thermoelectric unit, electromotive force, current, and output power distribution along the flow direction, under different circuit layouts. In addition, the power output performance of different circuit layouts, including the full-series-type and multi-stage-series types, are compared. The results indicate that the multi-stage series circuit layout can achieve a higher output power, and the higher the stage number, the higher the power output; however, the increased range becomes significantly smaller. Considering the complexity and connection of the circuit control, the recommended segment number of the multistage series type is three.

Keywords: circuit layout; full series type; multi-stage series type; thermoelectric generation; output power

1. INTRODUCTION

Semiconductor thermoelectric power generation is a technology based on the Seebeck effect of thermoelectric materials to directly convert heat energy into electricity because it is an all-solid energy conversion mode with the traditional power generation technology, this technology has no pollution, no noise, no moving parts, high reliability, prominent advantages, combined with energy storage device which can realize continuous production [1-3]. However, owing to its relatively low thermoelectric conversion efficiency, its wide applicability is limited. Considering that waste heat is a resource of low cost or even no cost, low thermal power conversion efficiency is no longer a major problem; our focus is now on obtaining a higher output power of the generator [4].

In recent years, several scholars have conducted research on thermoelectric materials and structural optimization. In thermoelectric materials, Haider Ali et al. [5] utilized the improved P- and N-type materials to achieve efficiency and power output with different external load parameters. The dimensionless temperature was analyzed, and the results indicated that the thermal efficiency decreased with an increase in the temperature, dimensionless parameter, and peak power in lower values of the external load parameters. In terms of efficient thermoelectric module design, there have been a number of articles published on thermoelectric unit groups. Numerical models of thermoelectric modules, such as Jun Wang [6] and others consider the open circuit voltage, output power, and the number of thermocouples, aiming at efficiency and output power. Furthermore, the analyses of the internal resistance vary with the temperature and thermoelectric leg length of the hot end or the change in the diameter. The results indicate that when the temperature of the hot end is constant, with a decrease

Selection and peer-review under responsibility of the scientific committee of CUE2021

in the cross-sectional area, the internal resistance, open circuit voltage, and efficiency increase; however, the output power is reduced. When the cross-sectional area is constant, the open-circuit voltage, output power, and efficiency increase with an increase in hot-side temperature. Fabian-Mijangos et al. [7] considered the output power of symmetric and asymmetric modules as a function of load resistance for the trapezoidal leg thermoelectric module, and observed that compared with the conventional thermoelectric module with a constant square cross section, the asymmetric thermoelectric module exhibited almost twice the thermoelectric quality factor. Rezania et al. [8] focused on a single pair of PN junction thermoelectric elements, optimized the ratio of the cross-sectional area of P-type and N-type semiconductors, and pointed out that because of the lower resistance and higher thermal conductivity of N-type materials, when the area of N-type materials is smaller than that of P-type materials, a higher energy will be generated. Dongxu et al. [9] conducted an experimental analysis of three thermo–electric modules with different geometries and verified the model experimentally. In addition, the effects of the number of legs on the output power and efficiency of the thermoelectric module were studied. The results indicate that the power output increases monotonously with an increase in the number of thermoelectric legs, and the efficiency first increases, and then decreases with an increase in the number of thermoelectric legs. Meng et al. [10] proposed the spiral structure, the results showed that the spiral module can produce higher output power. It can be noted that several important research results have been achieved in the optimization of thermoelectric modules. It should be noted that the current thermoelectric module mainly focuses on the structural optimization of the PN leg shape, thermoelectric leg length, and leg area. The minority literature considers the effect of circuit layout on the performance of thermoelectric output performance. Therefore, this study introduces two types of circuit layouts, the full series type and multi-stage series type, for the engine exhaust thermoelectric generator, and the internal temperature and electrical performance are compared. Finally, the optimal circuit layout is obtained to achieve high thermoelectric power conversion.

2. THERMOELECTRIC MODEL

2.1 Model formulation

The overall structure of the TEG is illustrated in Fig. 1. The engine exhaust heat exchanger channel was placed between the two thermoelectric modules; it served as a heat source for the two thermoelectric modules. The cooling water heat transfer channel was arranged at the other end of the thermoelectric module, which served as the cold source of the thermoelectric module.

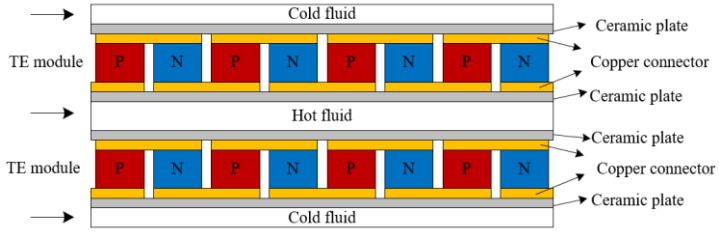

Fig. 1 Overall structure of thermoelectric generator

Fig. 2 illustrates the schematic diagram of a series circuit layout for the thermoelectric generator. In the figure, there are N_x thermoelectric units in total along the *x* direction (exhaust flow direction), and N_y units in the *y* direction (across flow direction). Along x direction, the N_x thermoelectric units are equally divided into *w* series circuits, and the number of thermoelectric units in each series block is n_x. It is called full series circuit layout when $w = 1$, and multi-stage series circuit layout when $w > 1$. All the output circuits produced by thermoelectric modules are connected to a storage battery to collect the conversion power.

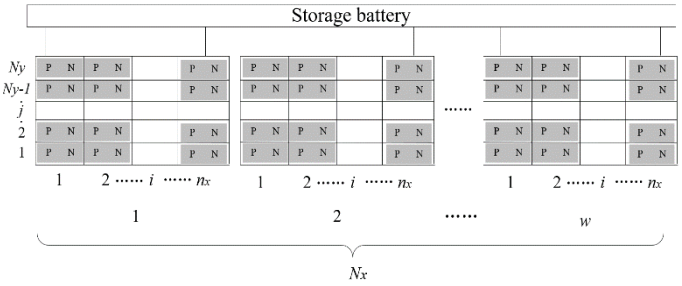

Fig. 2 Schematic diagram of series circuit layout for thermoelectric generator

All the thermoelectric units included in similar series circuits form one thermoelectric module containing $n_x \times N_y$ PN pairs. The coordinates (i, j) represent the PN pair number of lines and rows, respectively, in each module, where I = 1 to n_x, and j = 1 to N_y.

The heat transfer equilibrium equations for the ith finite calculation element can be described as in [11]:

$$\begin{aligned} q_h^i &= 0.5c_f m_f (T_f^i - T_f^{i+1}) = n_y \left[\alpha_{pn} I T_h^i + K_{pn}(T_h^i - T_L^i) - 0.5I^2 R_{pn} \right] \\ &= n_y ab \left[0.5\left(T_f^i + T_f^{i+1}\right) - T_h^i \right] / \left(R_{f1} + R_{f2} + R_{f3}\right) \\ q_L^i &= 0.5c_c m_c (T_c^{i+1} - T_c^i) = n_y \left[\alpha_{pn} I T_L^i + K_{pn}(T_h^i - T_L^i) + 0.5I^2 R_{pn} \right] \\ &= n_y ab \left[0.5\left(T_c^i + T_c^{i+1}\right) - T_h^i \right] / \left(R_{c1} + R_{c2} + R_{c3}\right) \end{aligned} \quad ,(1)$$

where c_f and c_c are the specific heat capacities of the hot and cold fluids, respectively; m_f and m_c are the total mass flow rates of the hot and cold fluids, respectively; α_{pn} denotes the Seebeck coefficient, K_{pn} represents the thermal conductance, and R_{pn} indicates the electric resistance for a P–N semiconductor couple. These can be obtained as

$$\alpha_{pn} = \alpha_p - \alpha_n \quad (2)$$

$$K_{pn} = c_1 c_2 (\lambda_p + \lambda_n) / c_3 \quad (3)$$

$$R_{pn} = c_3 (\rho_p + \rho_n) / (c_1 c_2), \quad (4)$$

where α_p, ρ_p, λ_p, α_n, ρ_n, and λ_n are the Seebeck coefficient, resistivity, and thermal conductivity, respectively, of the P-type and N-type legs; c_1, c_2, *and* c_3 are the length, width, and height of the semiconductor leg, respectively, for both the P- and N-type exchangers.

According to the Seebeck effect, the electromotive force produced by the i-line PN pairs can be represented by:

$$E_i = n_y \alpha_{pn} (T_f^i - T_c^i), \quad (5)$$

where, $T_f(i)$ and $T_c(i)$ are the temperatures of the hot and cold fluids of the thermoelectric units, respectively.

Current in the circuit can be represented by

$$I = \left(\sum_{i=1}^{n_x} E_i \right) / \left(2 n_x n_y R_{pn} \right). \quad (6)$$

Output power on each column of the i line, and total output power can be represented by

$$P_i = E_i I - I^2 R_{pn} n_y \quad (7)$$

$$P_{teg} = 2 \sum_{i=1}^{n_x} P_i \quad . \quad (8)$$

h_c is the convective heat transfer coefficient of cooling water.

The physical properties of air were adopted as the physical parameters of the thermal fluid. An HZ-20 commercial thermoelectric module was utilized. Fortran programming was utilized as the calculation method. The basic calculation parameters for the thermoelectric system are listed in Table 1.

Table 1 Basic calculation parameters of the thermoelectric system

Item	Value	Item	Value
c_1(m)	0.005	m_f(g s^{-1})	30
c_2(m)	0.005	m_c(g s^{-1})	500
c_3(m)	0.003	T_c^1(°C)	80
h_c(W m^{-2} K^{-1})	1000	T_f^1(°C)	500
α_P(V K^{-1})	2.037×10^{-4}	α_N(V K^{-1})	-1.721×10^{-4}
ρ_p (S m^{-1})	1.314×10^{-5}	ρ_n (S m^{-1})	1.119×10^{-5}
λ_p (W m^{-1} K^{-1})	1.265	λ_n (W m^{-1} K^{-1})	1.011

2.2 Model validation

To verify the reliability of the calculation results of the established mathematical model, a comparison between the simulation calculation results and the experimental results is illustrated in Fig. 3.

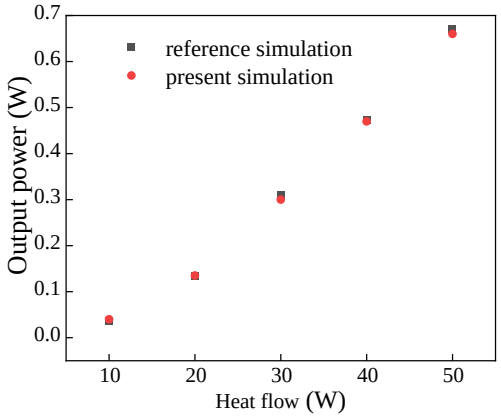

Fig. 3 Comparison between simulation results and experimental results

In Fig. 3, the calculation results obtained by this program are compared with the experimental data in the literature [12]. In the experiment, a heater with a heating area of 40 mm^2 was set at the hot end of the thermoelectric module, and the test heat flow Q_h was 10, 20, 30, 40, and 50 W respectively. The type of thermoelectric module selected in the test was teg1-127-1.4-1.6, the structural size was 40 mm × 40 mm × 3.8 mm, and the cooling mode was water cooling.

In the simulation calculation, similar thermoelectric conditions, and physical parameters as those in the literature were adopted to calculate the thermoelectric output power under different heat flows. Evident from the comparison between the calculated data obtained from the self-built model and the experimental data in the literature, the error between the simulated calculation results and the experimental results is less than 2%, which verifies the accuracy of the model established in this study, and the self-written calculation program.

3. RESULTS AND DISCUSSION

3.1 Internal Temperature distribution performance

A thermoelectric generator with a total of N_y = 56, and N_x = 60 was utilized. Two different circuit layout connections, full-series-type and two-stage series-type, are compared here. Fig. 4 illustrates the temperature distribution of the hot and cold ends of the thermoelectric unit, under two different circuit layout connections. It is evident that the temperature distributions of the two circuit layout connection modes are not similar. Compared with the full series circuit, the hot fluid temperature $T_f(i)$ decreases, and the cold fluid temperature $T_c(i)$ increases in the first section of the segmented series circuit, while the hot fluid temperature $T_f(i)$ increases, and the cold fluid temperature $T_c(i)$ decreases in the second section.

The temperature difference distribution of the hot and cold ends of the thermoelectric unit, under two different circuit layout connection modes, is illustrated in Fig. 5. Compared with the full series circuit, the temperature difference of the first section decreases, while that of the second section increases for the two-stage series circuit mode. A decrease in the temperature leads to a decrease in power generation. Therefore, a decrease in the temperature in the previous section of the segmental series circuit will have a negative effect to power output, while a rise in temperature difference in the latter section will have a favorable effect.

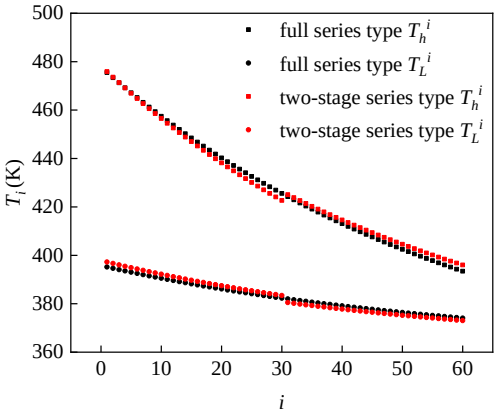

Fig. 4 Temperature distribution along the circuit under a different circuit layout

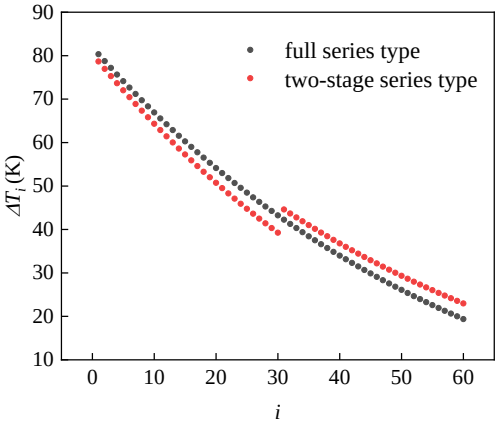

Fig. 5 Temperature difference distribution of cold and hot ends under a different circuit layout

3.2 Internal current and electromotive force performance

To explore the influence of the circuit layout on the internal thermoelectric performance, Figs. 6, 7, and 8 respectively illustrate the distributions of the internal electromotive force, current, and power output of the ith thermoelectric unit along the flow direction, for the full series and two-stage series modes. Fig. 6 illustrates that the electromotive force decreases continually along the flow direction for the full series type. This is caused by the decrease in the temperature between the hot and cold ends of the thermoelectric module. For the two-stage series circuit mode, the electromotive force of the first section is lower than that of the full series circuit, whereas the second section is higher than that of the full series circuit. It is determined by the temperature difference distribution performance, as illustrated in Fig. 4 and 5. Fig. 7 illustrates the internal

current distribution. From this, it can be seen that the internal currents are quite different for each segment of the two-stage circuit layout mode. Moreover, compared with the current of the full-seriousness mode, the current of the first segment is higher, and the second segment is lower. The extent of increase in the first segment is larger than the decrease in current in the second segment. This is determined by the internal coupling performance of the electromotive force and electric resistance.

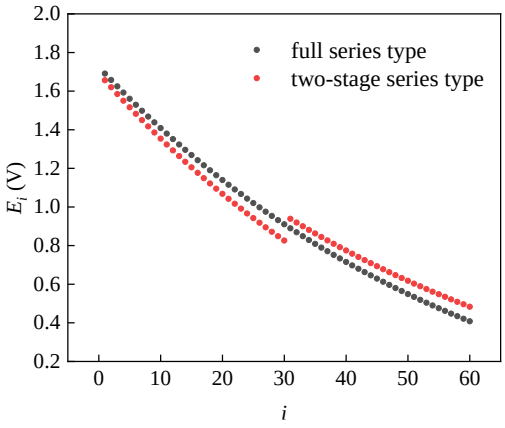

Fig. 6 Electromotive force distribution under different circuit layout

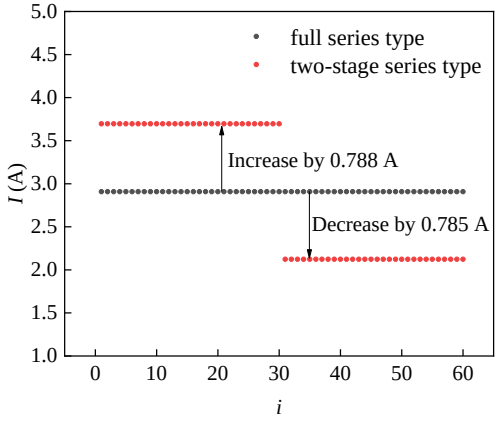

Fig. 7 Current distribution under different circuit layout

3.3 Output power performance

Based on the internal thermal and electrical performance analyses above, the power output produced by the ith line of thermoelectric units for different circuit layouts is illustrated in Fig. 8. It can be observed that the total power output of the two-stage series mode (covered area PS21 + PS22) is significantly higher than that of the full series circuit (covered area PS11 + PS12). The total output power of the full series type is 82.97 W, and the total output power of the two-stage series type is 89.13 W. Compared with full series type, the total power of the first stage is reduced by 2.43 W, and the total power of the second stage is increased by 8.59 W. Overall, it was the second segment that achieved the overall power increase.

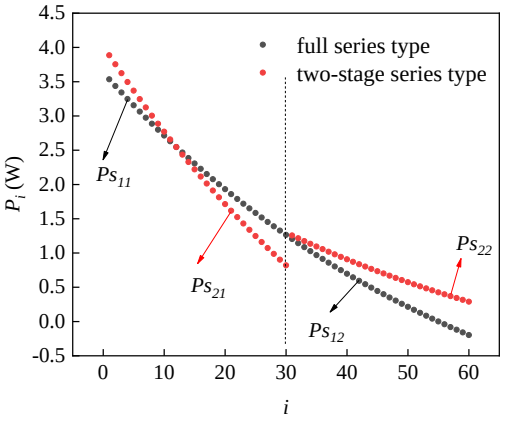

Fig. 8 Power distribution along the circuit under different circuit layout

Fig. 9 illustrates the distribution of the total output power for different multistage series circuit modes. It can be observed that with an increase in the series number of segments, the output power of the thermoelectric generator increases continuously compared to the full series mode, but the rate of increase becomes increasingly smaller with the increase in series segment number. When the number of segments is increased to three, the increase in the output power is gradually slower than in the full series type. Considering the complications of the multi-stage thermoelectric control, the recommended segment number is three.

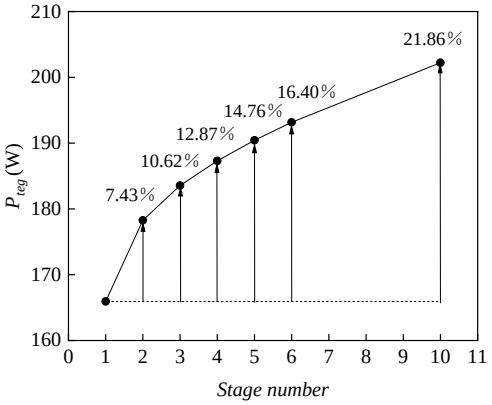

Fig. 9 Output power at different multi-stage series mode

4. CONCLUSION

In this study, the effect of the circuit connection mode on the thermoelectric performance was studied by comparing the full series mode and multi-stage series mode with the aid of Fortran software. The following conclusions were drawn:

(1) The internal thermoelectric distribution characteristics, including temperature, electromotive force, current, and power, are significantly different for the full-and multi-stage series modes. Considering the number of segments as two as an example, it was determined that the temperature difference between the hot and cold ends, and the electromotive force of the first segment for the two-stage series circuit is lower than that of the full series mode, and it is higher for the second segment. However, the current exhibits an adverse change trend. Finally, compared with the full series mode, the power contribution of the second section is greater.

(2) The internal thermal-electrical distribution characteristics determined the total power output performance of the TEG. The greater the number of segments of the multi-stage series circuit, the greater the total output power. However, when the number of segments increases by more than three, the increase in the output power becomes increasingly limited. Therefore, a three-stage series circuit is recommended by considering both the higher output power and easy circuit control in application for this study. Finally, it is meaningful to achieve a high power output of the TEG by designing a reasonable circuit connection mode.

ACKNOWLEDGEMENTS

The authors are grateful for financial support from the National Natural Science Foundation of China (51806152), the International Cooperation Program of the Ministry of Science and Technology of China (2017YFE0198000), and the Tianjin Natural Science Foundation (No.18JCZDJC97100).

REFERENCE

[1] Poudel B, Hao Q, Ma Y, Lan Y, Minnich A, Yu B, High-thermoelectric performance of nanostructured bismuth antimony telluride bulk alloys. Science 2008; 320(5876): 634-638.

[2] Ming T, Pan T, Wang Q, Zhou J, Yang W, Gong T. The influence of non-uniform heat flux on the performance of thermoelectric devices. CIESC Journal 2016; 67(05):172-179.

[3] Eddine A, Chalet D, Faure X, Aixala L, Chesse P. Effect of engine exhaust gas pulsations on the performance of a thermoelectric generator for wasted heat recovery: An experimental and analytical investigation. Energy 2018; 162:715-727.

[4] Liang G, Zhou J, Huang X. Analytical model of parallel thermoelectric generator. Appl. Energy 2011; 88(12):5193-5199.

[5] Ali H, Yilbas B. Influence of pin material configurations on thermoelectric generator performance. Energy Conv. Manag. 2016; 129:157-167.

[6] Wang J, Li Y, Zhao C, Cai Y, Zhu L, Zhang C. An optimization study of structural size of parameterized thermoelectric generator module on performance. Energy Conv. Manag. 2018; 160:176-181.

[7] Fabian-Mijarigos A, Min G, Alvarez-Quintana J. Enhanced performance thermoelectric module having asymmetrical legs. Energy Conv. Manag. 2017; 148:1372-1381.

[8 Rezania A, Rosendahl L, Yin, H. Parametric optimization of thermoelectric elements footprint for maximum power generation. J. Power Sources 2014; 255-151-6.

[9] Ji D, Wei Z, Pou J, Mazzoni S, Rajoo S, Romagnoli A. Geometry optimization of thermoelectric modules: simulation and experimental study. Energy Conv. Manag. 2019; 195:236-243.

[10] Meng X, Suzu K, Ryosuke O. Helical configuration for thermoelectric generation. Appl. Therm. Eng. 2016; 99:352-357.

[11]Sahin A, Yilbas, B. Thermodynamic irreversibility and performance characteristics of thermoelectric power generator. Energ. 2013; 55:899-904.

[12]Zhou Z, Zhu D, Wu H, Zhang H. Modeling, Experimental Study on the Heat Transfer Characteristics of Thermoelectric Generator. J. Therm. Sci. 2013; 22(1):48-54.